N91-21084

COMPUTATION OF TURBULENT HIGH SPEED MIXING LAYERS USING A TWO-EQUATION TURBULENCE MODEL

J.R. Narayan
Research Scientist
Analytical Services and Materials, Inc., Hampton, Virginia.
and
B. Sekar
Research Scientist
Vigyan Research Associates, Inc., Hampton, Virginia.

ABSTRACT

A two-equation turbulence model has been extended to be applicable for compressible flows. A compressibility correction based on modelling the dilatational terms in the Reynolds stress equations has been included in the model. The model is used in conjunction with the SPARK code for the computation of high-speed mixing layers. The observed trend of decreasing growth rate with increasing convective Mach number in compressible mixing layers is well predicted by the model. The predictions agree well with experimental data and the results from a compressible Reynolds stress model. The present model appears to be well suited for the study of compressible free shear flows. Preliminary results obtained for reacting mixing layers have also been included.

NOMENCLATURE

b_i	body force of species i
C_1, C_2, C_μ	turbulence model constants
c_p	specific heat at constant pressure
c_{p_i}	c_p for i^{th} species
D_{ij}	binary diffusion coefficient
D_T	thermal diffusion coefficient
E	total internal energy
f_i	mass fraction of species i
$\mathbf{H}$	source vector
H	total enthalpy
h	static enthalpy
h_i	enthalpy of species i
h_i^o	reference enthalpy of species i
k	turbulent kinetic energy
M_i	molecular weight of species i
M_t	Turbulent Mach number
ns	number of chemical species
Pr, Pr_t	laminar and turbulent Prandtl numbers
p	pressure
$\vec{q}$	heat flux vector
R^o	universal gas constant

Sc, Sc_t	laminar and turbulent Schmidt numbers
T	temperature
t	time
Δt	time step
$\mathbf{U}$	dependent variable vector
$\vec{U}$	velocity vector
$\vec{V_i}$	diffusion velocity vector of species i
$\dot{w}_i$	species production rate of species i
X_i	mole fraction of species i
x	streamwise coordinate
x_j	j^{th} coordinate
y	transverse coordinate
α	compressibility correction coefficient
γ	ratio of specific heats
δ_{ij}	Kronecker delta
ϵ	dissipation rate
ϵ_c	compressible dissipation rate
κ	thermal conductivity
λ	second viscosity coefficient
μ	laminar viscosity
μ_t	turbulent viscosity
ν	kinematic viscosity
ρ	density
$\sigma_k, \sigma_\epsilon$	turbulence model constants
τ_{ij}	stress tensor
Φ_j	flux vector in j^{th} direction

Subscripts

a	high speed stream
b	low speed stream
t	turbulent quantity

INTRODUCTION

In recent years, the development of an airbreathing hypersonic vehicle has received considerable attention. This is a complex task and requires innovative research in many technical areas such as aerodynamics, propulsion, structures and materials. Development of viable propulsion systems for such a vehicle is being pursued at numerous research institutions around the country. One such program is being carried out at the NASA Langley Research Center in which a highly integrated, hydrogen-fueled supersonic combustion ramjet (scramjet) engine is envisioned to be a viable propulsion system for hypervelocity vehicles [1,2]. Due to the complex nature of such a task, numerous research programs have been initiated. One of these research efforts is concerned with understanding the details of the complex flow field inside the engine and evaluating its main features for a range of flow conditions. The work reported here is concerned with this effort in which computational analysis of the scramjet flow field is carried out.

The flow field in the scramjet combustor is highly complex. It is governed by the Navier-Stokes equations coupled with a system of equations describing the chemical reactions that occur. The flow is expected to be turbulent in most part of the combustor. This requires that the analysis be capable of addressing compressible turbulent reacting flows. The interaction between turbulence and chemical reactions is an important issue in the analysis. The presence of turbulence in any flow complicates accurate analysis of the flow due to the wide range of length and time scales. Exact solution of complex flows, such as that in a scramjet combustor, is impossible at present because of these turbulence scales. Hence some form of simplified treatment of the turbulence is mandatory in such problems and turbulence models are used in

this regard. Establishing turbulence models that are suitable for flows such as that of the scramjet is very difficult since the effects of turbulence on the flow as a whole and on the chemical reactions in particular are not well understood. The model should be accurate enough in predicting the physics of the problem without increasing the complexity of the solution procedure any more than is necessary.

A variety of turbulence models, which have been used for many different flow configurations, exist today. These models range from the simplest mixing-length or zero-equation models to the most general Reynolds stress closures. Also, other means of analyzing turbulent flows, such as large eddy simulation, are being developed. A useful review of the field was conducted by Nallasamy [3]. One class of models that is widely used in turbulence computations today is the two-equation model. In this model, a differential equation for the mean turbulent kinetic energy and another for some form of the length scale of turbulence are solved along with the averaged forms of the Navier-Stokes equations. These two-equation models have been used with some degree of success for many engineering problems. They are relatively easy to implement in a given solution procedure and are computationally economic in comparison with the more general Reynolds stress models. These models do have their limitations and their applicability to any flow problem must be validated before using them. One of the major restrictions of most of the turbulence models in use today is that they have been developed for incompressible flows. Adhoc modifications to account for compressibility have been made to some of these models. A discussion on this subject is given by Yang et al. [4]. A fully compressible turbulence model of the two-equation and higher order does not exist because the averaged equations for compressible flows are not easily amenable to modelling using any of the known techniques. However, good progress has been made in this area by many researchers and it is hoped that turbulence models applicable to compressible flows should soon be available. In the present analysis, a two-equation model of turbulence has been used with a compressibility correction derived from the Reynolds stress closure model of Sarkar et al. [5]. The two turbulence variables are the turbulent kinetic energy and its dissipation rate. The governing equations are Favre averaged [6] thus including the effects of mean density variations. At present, the model does not include the turbulence-chemical reactions interactions and all the model constants of the incompressible model [7] are retained.

The two-equation model is tested on a spatially developing, primarily supersonic, chemically reacting plane mixing layer. A major portion of the chemical reactions in the scarmjet combustor occur in mixing layers and all the complexities introduced by fluid mechanics, combustion chemistry and the interaction between them are retained by the reacting mixing layer. A detailed discussion on this topic is given by Drummond et al. [1]. Mixing layers have been studied extensively over the years. Some of the earlier work in this area is found in reference [8], which resulted after the conference on free shear flows held at NASA Langley Research Center in 1972, and in reference [9], in which the density effects on subsonic mixing layers have been discussed. Reference [10] gives a good picture of recent developments in the area of turbulent shear flows of which the mixing layer is a subset. However, as with many other compressible flows, reliable experimental data in the area of reacting mixing layers is limited. Availability of reliable experimental data for the purpose of validation is crucial in the development of turbulence models and the lack of this data is one of the reasons why models applicable to reacting flows are not common today.

In the present work, the two-equation model is applied to the high-speed plane mixing layer problem over a wide range of flow conditions without and with chemical reaction. The nonreacting cases are computed for air-air systems. Hydrogen-air combustion models are used for the reacting flows. Single-step and multiple-step reaction systems are used here. The two gas streams that form the mixing layer are supersonic whereas the convective Mach number [11] of the layer varies from subsonic to supersonic values. The computer code SPARK, developed at the NASA Langley Research Center [12], has been used. It solves the governing equations using a fourth order compact scheme. The mean flow variables such as velocity, internal energy, the two turbulence variables and the concentrations of various species such as hydrogen, oxygen, nitrogen etc., are computed. Representative results are presented and pertinent flow features are discussed. The predictions have been compared with those of a Reynolds stress closure [13,14] and also with available experimental data [11,15,16,17]. Major flow characteristics such as the growth rate of the mixing layer, mean velocities, turbulent kinetic energy etc., are used for comparisons.

411

GOVERNING EQUATIONS

The Navier-Stokes equations along with equations for energy and species continuity which govern flows with multiple species undergoing chemical reaction have been used [18]. These governing equations are

Continuity

$$\frac{\partial \rho}{\partial t} + \nabla \cdot (\rho \vec{U}) = 0 \tag{1}$$

Momentum

$$\frac{\partial (\rho \vec{U})}{\partial t} + \nabla \cdot (\rho \vec{U} \vec{U}) = \nabla \cdot \tau + \rho \sum_{i=1}^{ns} f_i \vec{b}_i \tag{2}$$

where

$$\tau \equiv \tau_{ij} = -p\, \delta_{ij} + \mu \left(\frac{\partial u_i}{\partial x_j} + \frac{\partial u_j}{\partial x_i} \right) + \lambda \frac{\partial u_k}{\partial x_k} \delta_{ij} \tag{3}$$

with repeated indices indicating summation.

Energy

The total energy(kinetic + internal) is chosen as the dependent variable in the energy equation, given as

$$\frac{\partial (\rho E)}{\partial t} + \nabla \cdot (\rho \vec{U} E) = \nabla \cdot (\tau \cdot \vec{U}) - \nabla \cdot \vec{q} + \rho \sum_{i=1}^{ns} f_i \vec{b}_i (\vec{U} + \vec{V}_i) \tag{4}$$

where, neglecting radiation heat transfer,

$$\vec{q} = -\kappa \nabla T + \rho \sum_{i=1}^{ns} h_i f_i \vec{V}_i + R^o T \sum_{i=1}^{ns} \sum_{j=1}^{ns} \left(\frac{X_j D_{T_i}}{M_i D_{ij}} \right)(\vec{V}_i - \vec{V}_j) \tag{5}$$

Species Continuity

$$\frac{\partial (\rho f_i)}{\partial t} + \nabla \cdot (\rho \vec{U} f_i) = \dot{w}_i - \nabla \cdot (\rho f_i \vec{V}_i) \tag{6}$$

Also,

$$E = \sum_{i=1}^{ns} h_i f_i - \frac{p}{\rho} + \frac{u_k u_k}{2} \tag{7}$$

with repeated indices indicating summation in the kinetic energy term.

$$h_i = h_i^o + \int_{T_r}^{T} c_{p_i} dT \qquad i = 1, 2, ..., ns \tag{8}$$

$$p = \rho R^o T \sum_{i=1}^{ns} \frac{f_i}{M_i} \tag{9}$$

The diffusion velocities are found by solving

$$\nabla X_i = \sum_{j=1}^{ns} \frac{X_i X_j}{D_{ij}} (\vec{V}_j - \vec{V}_i) + (f_i - X_i) \frac{\nabla p}{p} + \frac{\rho}{p} \sum_{j=1}^{ns} f_i f_j (\vec{b}_i - \vec{b}_j) +$$

$$\sum_{j=1}^{ns} \frac{X_i X_j}{\rho D_{ij}} \left(\frac{D_{Tj}}{f_j} - \frac{D_{Ti}}{f_i} \right) \frac{\nabla T}{T} \tag{10}$$

412

Note that if there are ns chemical species, then $i = 1, 2, ..., (ns - 1)$ and $(ns - 1)$ equations must be solved for the species f_i. The final species mass fraction f_{ns} can then be found by conservation of mass since $\sum_{i=1}^{ns} f_i = 1$.

The procedures for evaluating quantities such as the specific heats, equilibrium constant for the chemical reactions, etc., are described in reference [1]. Also, details regarding the chemistry models, thermodynamic models and the diffusion models are found in reference [1].

Averaged Governing Equations

Density-weighted averaging (also known as Favre-averaging [6]) is used to derive the equations which describe the fully turbulent flow from the above set of equations. The dependent variables, except density and pressure, are written in the form,

$$\phi = \tilde{\phi} + \phi''$$ (11)

where the Favre-mean $\tilde{\phi}$ is defined as

$$\tilde{\phi} \equiv \frac{\overline{\rho \phi}}{\overline{\rho}}$$ (12)

In this equation, the overbar indicates conventional time-averaging. Density and pressure are split in the conventional sense as,

$$\rho = \overline{\rho} + \rho' \quad \text{and} \quad p = \overline{p} + p'$$ (13)

The following relations exist in this form of time-averaging:

$$\begin{aligned}
\overline{\phi''} &= -\frac{\overline{\rho' \phi'}}{\overline{\rho}} \\
\overline{\rho \phi''} &= 0 \\
\overline{\phi'} &= 0
\end{aligned}$$ (14)

The averaged continuity and momentum equations are

$$\frac{\partial \overline{\rho}}{\partial t} + \frac{\partial \overline{\rho} \tilde{U_i}}{\partial x_i} = 0$$ (15)

$$\frac{\partial \overline{\rho} \tilde{U_i}}{\partial t} + \frac{\partial \overline{\rho} \tilde{U_i} \tilde{U_j}}{\partial x_j} = -\frac{\partial \overline{p}}{\partial x_i} - \frac{\partial \overline{\rho u_i'' u_j''}}{\partial x_j} + \frac{\partial \overline{\tau_{ij}}}{\partial x_j}$$ (16)

The total energy E can be written in terms of the total enthalpy(H) as

$$E = H - \frac{p}{\rho}$$ (17)

Rewriting the energy equation (4) using the above and time-averaging,

$$\frac{\partial (\overline{\rho} \tilde{H} - \overline{p})}{\partial t} + \frac{\partial (\overline{\rho} \tilde{H} - \overline{p}) \tilde{U_j}}{\partial x_j} = -\frac{\partial}{\partial x_j}(\overline{p} \tilde{U_j} + \overline{\rho u_j'' H''}) - \frac{\overline{\partial Q_j}}{\partial x_j} + \frac{\overline{\partial u_i \tau_{ij}}}{\partial x_j}$$ (18)

In the above equations the body forces contribution has been omitted. Also, $\overline{Q_j}$ represents the averaged heat flux term (equation (5)). The species continuity equation (6) is averaged similarly to get,

$$\frac{\partial \overline{\rho} \tilde{f_i}}{\partial t} + \frac{\partial \overline{\rho} \tilde{f_i} \tilde{U_j}}{\partial x_j} = \overline{w_i} - \frac{\partial}{\partial x_j}(\overline{\rho u_j'' f_i''} + \overline{\rho f_i (V_i)_j})$$ (19)

413

In this equation, the term $\dot{w}_i$ contains correlations which have not been included in the present model.

The equations for the two turbulence variables, turbulent kinetic energy (k) and the energy dissipation rate (ϵ), are derived by suitably manipulating the momentum and continuity equations (equations (2) and (1)) and utilizing equations (11) – (14). Defining k and ϵ as

$$k \equiv \frac{\overline{\rho u_i'' u_i''}}{2\overline{\rho}} \tag{20}$$

$$\epsilon \equiv \frac{\overline{\rho \nu \frac{\partial u_i''}{\partial x_j} \frac{\partial u_i''}{\partial x_j}}}{\overline{\rho}} \tag{21}$$

the equation for the turbulent kinetic energy can be written as

$$\frac{\partial \overline{\rho} k}{\partial t} + \frac{\partial \overline{\rho} k \widetilde{U_j}}{\partial x_j} = -\overline{\rho u_i'' u_j''} \frac{\partial \widetilde{U_i}}{\partial x_j} - \overline{\tau_{ij} \frac{\partial u_i''}{\partial x_j}} - \overline{u_i''} \frac{\partial \overline{p}}{\partial x_i} + \overline{p' \frac{\partial u_i''}{\partial x_i}}$$
$$- \frac{\partial}{\partial x_j} \left(\overline{\rho u_i'' u_i'' u_j''} + \overline{p' u_i''} \, \delta_{ij} - \overline{u_i'' \tau_{ij}} \right) \tag{22}$$

Substituting for τ_{ij} and rearranging terms,

$$\frac{\partial \overline{\rho} k}{\partial t} + \frac{\partial \overline{\rho} k \widetilde{U_j}}{\partial x_j} = -\overline{\rho u_i'' u_j''} \frac{\partial \widetilde{U_i}}{\partial x_j} - \mu \overline{\frac{\partial u_i''}{\partial x_j} \frac{\partial u_i''}{\partial x_j}} - \frac{\partial}{\partial x_j} \left(\overline{\rho u_i'' u_i'' u_j''} + \overline{p' u_i''} \, \delta_{ij} \right)$$
$$+ \frac{\partial}{\partial x_j} \left(\bar{\mu} \frac{\partial k}{\partial x_j} \right) - \overline{u_i''} \frac{\partial \overline{p}}{\partial x_i} + \overline{p' \frac{\partial u_i''}{\partial x_i}} + \Theta \tag{23}$$

where Θ is a set of molecular diffusion-like terms which can be neglected in high Reynolds number flows [4]. The first term on the right hand side of equation (23) is the energy production term, the second one is the dissipation term (21), the third and fourth terms represent diffusion of the turbulent energy and the next two terms represent the effect of compressibility.

The equation for the dissipation rate (ϵ) can be derived in a similar manner. It is not included here because it is quite long and the current model uses a simplified form of this equation. However, the modelled form of this equation, which has been used in the computations, will be included later in this report.

Modelled Equations

The k-ϵ model achieves closure of the equations governing the turbulent flows by invoking the Boussinesq approximation which relates the turbulent stresses (Reynolds stresses) to the mean strain rate. Thus, the Reynolds stress tensor is written as,

$$-\overline{\rho u_i'' u_j''} = \mu_t \left(\frac{\partial \widetilde{U_i}}{\partial x_j} + \frac{\partial \widetilde{U_j}}{\partial x_i} \right) - \frac{2}{3} \overline{\rho} k \, \delta_{ij} \tag{24}$$

where μ_t is the turbulent/eddy viscosity defined in terms of some characteristic length and velocity scales. Here the length is taken to the turbulent length scale, $k^{\frac{3}{2}}/\epsilon$, and the velocity scale is assumed to be $k^{\frac{1}{2}}$ leading to the following expression for μ_t.

$$\mu_t = C_\mu \, \rho \frac{k^2}{\epsilon} \tag{25}$$

The correlations between the fluctuating velocity and the scalar fluctuations are modelled in a similar manner using a mean gradient hypothesis and a typical model is,

$$-\overline{\rho u_i'' \phi''} = \frac{\bar{\mu}_t}{\sigma_\phi} \left(\frac{\partial \widetilde{\phi}}{\partial x_i} \right) \tag{26}$$

414

where σ_ϕ is a coefficient which, normally, is a constant. For $\phi = f_i$, $\sigma_\phi = Sc_t$, and for the static enthalpy, $(\phi = h)$, $\sigma_\phi = Pr_t$.

Using the above, the averaged governing equations can be modified using models for the unknown correlations thus deriving a closed set of equations which can be solved. In this section, these modelled equations will be given. The mean continuity equation (15) does not require any further modelling. The momentum equation (16) has two terms (last two on the right hand side) that require modeling. The modelled momentum equation is,

$$\frac{\partial \bar{\rho} \widetilde{U_i}}{\partial t} + \frac{\partial \bar{\rho} \widetilde{U_i} \widetilde{U_j}}{\partial x_j} = -\frac{\partial \bar{p}}{\partial x_i} - \frac{\partial}{\partial x_j} \left[(\bar{\mu} + \mu_t)(\frac{\partial \widetilde{U_i}}{\partial x_j} + \frac{\partial \widetilde{U_j}}{\partial x_i}) - \frac{2}{3}(\bar{\mu}\frac{\partial \widetilde{U_k}}{\partial x_k} + \bar{\rho}k) \delta_{ij} \right] \tag{27}$$

The correlation $\overline{\rho u_j'' H''}$ in the thermodynamic energy equation (18) is split into its components here as

$$\overline{\rho u_j'' H''} = \overline{\rho u_j'' h''} + \frac{\overline{\rho u_i'' u_i'' u_j''}}{2} + \overline{\rho u_i'' u_j''} \, \widetilde{U_i} \tag{28}$$

The modelled energy equation then is,

$$\frac{\partial (\bar{p} \widetilde{H} - \bar{p})}{\partial t} + \frac{\partial (\bar{p} \widetilde{H} - \bar{p}) \widetilde{U_j}}{\partial x_j} = \frac{\partial}{\partial x_j} \left[(\frac{\bar{\mu}}{Pr} + \frac{\mu_t}{Pr_t}) \frac{\partial \widetilde{h}}{\partial x_j} + (\bar{\mu} + \frac{\mu_t}{\sigma_k}) \frac{\partial \widetilde{k}}{\partial x_j} \right]$$
$$+ \frac{\partial}{\partial x_j} (\overline{\tau_{ij}} - \bar{p}\,\delta_{ij} - \overline{\rho u_i'' u_j''}) \widetilde{U_i} \tag{29}$$

where σ_k is a coefficient that appears in the turbulent kinetic energy equation. The intermediate steps that lead to equation (29) are straight forward and hence are not included here. The modelled species continuity equation is

$$\frac{\partial \bar{p} \widetilde{f_i}}{\partial t} + \frac{\partial \bar{p} \widetilde{f_i} \widetilde{U_j}}{\partial x_j} = \overline{\dot{w}_i} - \frac{\partial}{\partial x_j} \left[(\frac{\bar{\mu}}{Sc} + \frac{\mu_t}{Sc_t}) \frac{\partial \widetilde{f}}{\partial x_j} \right] \tag{30}$$

Modelling of the turbulence terms in the equations is a major area of research by itself. Details of the modelling of the various terms are beyond the scope of this paper. Here the models used, along with the relevant references, will be given. The production term is exact in its form and does not need modelling. Modelling of the diffusion terms in the turbulent kinetic energy equation has been a well studied area and the model employed here is one of the most widely used [19]. The terms identified in the previous section as the compressibility terms are included in the present analysis since the flows considered are compressible. Recently, there has been a considerable amount of activity in the area of modelling these compressibility effects for various turbulence models. A short account of some of these modelling efforts can be found in reference [4]. Strahle [20] proposed a global compressibility correction for the turbulent kinetic energy equation. Recently, Sarkar et al. [5] proposed a model for the compressible dissipation in terms of the dissipation rate of turbulent kinetic energy and the local turbulent Mach number. This has been used in the present analysis as the model for the two compressibility terms in the turbulent kinetic energy equation. The compressible dissipation model is

$$\epsilon_c = \alpha M_t^2 \epsilon \tag{31}$$

Here M_t is the local turbulent Mach number defined as $M_t^2 = 2k/a^2$ where a is the local speed of sound and the model constant $\alpha = 1.0$. The modelled turbulent kinetic energy equation is [7]

$$\frac{\partial \bar{p} k}{\partial t} + \frac{\partial \bar{p} k \widetilde{U_j}}{\partial x_j} = -\overline{\rho u_i'' u_j''} \frac{\partial \widetilde{U_i}}{\partial x_j} - \bar{p}\epsilon(1 + \alpha M_t^2) + \frac{\partial}{\partial x_j}[(\bar{\mu} + \frac{\mu_t}{\sigma_k})\frac{\partial k}{\partial x_j}] \tag{32}$$

Modelling of the exact equation for the dissipation rate is extremely difficult, even for incompressible flows, due to the lack of understanding of the various complex correlation terms that are present. There have

been attempts at including some form of compressibility effects in the ϵ-equation [4] but no viable model has emerged so far. Hence, the incompressible form of the ϵ-equation is used in the present analysis [7]. The modelled form of this equation is

$$\frac{\partial \bar{\rho}\epsilon}{\partial t} + \frac{\partial \bar{\rho}\epsilon \widetilde{U_j}}{\partial x_j} = (C_1 \, P_k - C_2 \bar{\rho}\epsilon) \, \frac{\epsilon}{k} + \frac{\partial}{\partial x_j}[(\bar{\mu} + \frac{\bar{\mu}_t}{\sigma_\epsilon})\frac{\partial \epsilon}{\partial x_j}] \tag{33}$$

where P_k is the production term in the turbulent kinetic energy equation (first term on the right hand side of (32). This term can be written as

$$P_k = -\overline{\rho u_i'' u_j''} \frac{\partial \widetilde{U_i}}{\partial x_j}$$

$$= \bar{\mu}_t[\frac{1}{2}(\frac{\partial \widetilde{U_i}}{\partial x_j} + \frac{\partial \widetilde{U_j}}{\partial x_i})^2 - \frac{2}{3}(\frac{\partial \widetilde{U_k}}{\partial x_k})^2] - \frac{2}{3}\bar{\rho}k\frac{\partial \widetilde{U_k}}{\partial x_k} \tag{34}$$

The model constants used in the analysis are C_μ=0.09, C_1=1.44, C_2=1.92, σ_k=1.0, σ_ϵ=1.3, Pr=0.72, Pr_t=1.0, Sc=0.22 and Sc_t=1.0.

Solution of the Governing Equations

Once the governing equations and required modeling are in hand, the equations are discretized and integrated in space and time towards steady state solutions. The governing equations are written in vector form as follows.

$$\frac{\partial \mathbf{U}}{\partial t} + \frac{\partial \mathbf{\Phi}_j}{\partial x_j} = \mathbf{H} \tag{35}$$

where $\mathbf{U}$ is the vector of dependent variables, $\mathbf{\Phi}_j$ are flux vectors containing convective and diffusive terms (repeated indices indicate summation), and $\mathbf{H}$ are source terms containing production/dissipation terms in the equations. The temporally discrete form of equation (35) can then be written as

$$\mathbf{U}^{n+1} = \mathbf{U}^n - \Delta t \, [\frac{\partial \mathbf{\Phi}_j^n}{\partial x_j} - \mathbf{H}^{n+1}] \tag{36}$$

where n is the old time level and $n+1$ is the new time level. The flux terms are written at the old time level because the equations are advanced in real time at the smallest fluid time scale. The source terms in the k- and ϵ-equations are decoupled by suitable manipulation of the ratio ϵ/k in the present analysis. For example, in the k-equation, the dissipation term is written as,

$$\bar{\rho}\epsilon = \bar{\rho}k \, (\frac{\epsilon}{k}) \tag{37}$$

The term ϵ/k is treated as a known quantity taking its value from the previous time step in the solutions. A similar treatment of the source term is done for the ϵ-equation also. These nonlinear turbulence source terms are treated in a pointwise-implicit manner while solving the turbulence equations. The k- and ϵ-equations are written in the form,

$$(1 - \frac{\partial \mathbf{H}}{\partial \mathbf{U}}) \, (\mathbf{U}^{n+1} - \mathbf{U}^n) = - \Delta t \, [\frac{\partial \mathbf{\Phi}_j^n}{\partial x_j} - \mathbf{H}^n] \tag{38}$$

The jacobian $\frac{\partial \mathbf{H}}{\partial \mathbf{U}}$ can take different forms depending upon how the source terms are written. In the present computations, this jacobian has the following terms:

$$\frac{\partial H_k}{\partial \bar{\rho}k} = -[\frac{2}{3}D + \frac{\epsilon}{k} \, (1 + \alpha M_t^2)]$$

416

$$\frac{\partial H_k}{\partial \overline{\rho}\epsilon} = 0$$

$$\frac{\partial H_\epsilon}{\partial \overline{\rho}k} = 0$$

$$\frac{\partial H_\epsilon}{\partial \overline{\rho}\epsilon} = -[\frac{2}{3}C_1 D + C_2\frac{\epsilon}{k}] \tag{39}$$

where

$$D \equiv \frac{\partial U_j}{\partial x_j} \tag{40}$$

As an option, the chemical source term is also written implicitly [21] to alleviate the problem of stiffness in the governing equations when chemistry time scales become small as compared to fluid time scales early in a calculation or when the system approaches chemical equilibrium. The governing equations are written in two-dimensional cartesian form for the solutions. It must be pointed out here that even though turbulence is three-dimensional in nature, the contribution of the fluctuating velocity in the third dimension has not been incorporated in the calculations. The discretized equations are solved by means of the elliptic solver SPARK [12]. A fourth-order compact scheme is used in the solution procedure. Details of the code and the solution procedure can be found in [12].

RESULTS AND DISCUSSION

A two-dimensional, high-speed mixing layer is considered in this study. A schematic of this flow problem is given in figure 1. The two streams coming off the splitter plate are supersonic. However, the convective Mach number [11] of the mixing layer ranges from subsonic to supersonic values. The two streams are air for the nonreacting cases whereas the higher-speed stream is comprised of a hydrogen-nitrogen mixture (10% H_2 and 90% N_2) for the reacting mixing layer cases. The inlet mean velocity is assumed to have a hyperbolic tangent profile, thus imitating the flow that exists downstream of the splitter plate edge. Ease of computations prompted this choice of initial profile for the mean velocity. The initial distributions of the turbulent kinetic energy and its dissipation rate are chosen to be compatible with what is observed in such a flow problem. A constant turbulence intensity level is used in the free stream for arriving at the initial distribution of turbulent kinetic energy and the dissipation rate distribution is deduced from the k-field using a length scale parameter. These initial distributions are shown in figure 2. The temperature and pressure are assumed to be initially uniform for both the streams. The free stream turbulence intensity proved to be a sensitive parameter, especially for the supersonic convective Mach number cases. A constant value of the free stream turbulence intensity (with respect to the mean velocity) has been maintained in all the calculations. Hydrogen-oxygen reaction systems are considered in the reacting flow calculations since this solution procedure is to be applied to scramjet combustor flow studies. One-step (one reaction, four species) and multiple-step (eighteen reactions and nine species) reactions have been considered. Different sets of computations were done based on the convective Mach number of the mixing layer. Here, for a given free stream temperature and pressure, the slower speed stream had the same velocity in all the calculations changing only the speed of the faster stream in order to arrive at the required convective Mach number.

In this section, representative results of the calculations are presented. Comparison with available experimental data is done in a limited sense. Also, the solutions are compared with the Reynolds stress closure predictions carried out at NASA Langley [13,14]. Typical predictions of the mean velocity, temperature and turbulent kinetic energy for a convective Mach number of 1.5 are given in figure 3. The free stream Mach numbers of the two streams are 3.2 and 6.2. These figures show the development of the mixing layer in the axial direction and the corresponding changes in the flow variables. A slight shifting of the layer towards the lower speed stream is seen here. The mean temperature increases, from its free stream value, inside the mixing layer. A similar variation is observed in the turbulent kinetic energy distribution. Figure 4 shows the width of the mixing layer (vorticity thickness) as a function of the streamwise distance. Two values of the

convective Mach number have been considered. The growth of the layer is linear after the inital development of the flow and in this linear region, similarity in the mean flow characteristics can be expected. This is seen in figure 5 where the mean velocity and turbulent kinetic energy profiles are plotted in similarity variable coordinates. Here y_c represents the location where the two streams have a common boundary initially.

The major aim of the present work is to extend the widely used incompressible two-equation turbulence model for compressible flows. As mentioned earlier, a compressible correction has been incorporated in the turbulence model used here. The predicted growth rates of the mixing layer with and without the compressibility correction model are plotted in figure 6. For comparison, the results using a global correction model [20] are also included. Here C_δ is defined as,

$$C_\delta = \frac{d\delta}{dx} \frac{U_a + U_b}{U_a - U_b}$$

and C_{δ_0} is its value for incompressible flow (assumed to be at a convective Mach number of 0.1 here). The effect of compressibility on mixing layer is to reduce the growth rate of the layer with increasing convective Mach number. This trend is seen in the figure. For the cases without the compressibility correction and those with the global correction the growth rate seems to reach a constant value after a convective Mach number of about 0.5. However, the effects of compressibility are expected to be more pronounced beyond this point leading one to believe that the calculations without the above correction do not address the important problem of compressibility well. As seen in the figure, the effect of compressibility is well predicted by including the compressibility correction. This has been verified by comparing the predicted growth rate with available experimental data, as shown in figure 7. The growth rates predicted by means of the Reynolds stress closure[13] are also shown in this figure. As with any turbulent flow case, the experimental data here show a wide scatter [11,15,16,17]. This raises the question of whether the convective Mach number is the sole basis for comparison between the wide range of mixing layer data available in the literature. Setting aside this question for the moment, the figure shows that the trend of reduced growth rate with increasing convective Mach number is predicted very well by the k-ϵ model. The comparison between these predictions and the Langley experimental data is excellent in the supersonic range of the convective Mach number.

One of the important aspects of a two-equation model is that it is well suited for application in engineering flow problems from the point of view of ease of adaptability, computational economy etc. However, the model has been found to be lacking in certain flow cases where the Reynolds stress closure may be appropriate. So, one of the main steps in the present analysis has been to compare the k-ϵ predictions with the Reynolds stress closure predictions in order to evaluate its applicability to the flow problem considered. This is done in figure 8. Figure 8a compares the predicted mean axial velocity profiles at representative locations and figures 8b and 8c compare the turbulent kinetic energy and dissipation rate profiles, respectively. The comparisons show that the k-ϵ predictions agree very well with those of the Reynolds stress model [14] and hence for high-speed mixing layer flows applications the two-equation model seems to be suitable. However, it must be reiterated that this conclusion does not necessarily carry over to all compressible flow problems.

Coming back to the question of whether the convective Mach number should be the sole basis for comparing similar mixing layers, calculations were done with different free stream temperatures and velocities. Some of the results are shown in figure 9. In this figure, the free stream pressure is the same (1 atm) for cases 1 to 4 and it is increased by a factor of 2.1 for case 5. The results indicate some dependency of the growth rate on the free stream temperature. The figure also shows the equivalence between two sets of data (cases 1&5 and cases 2&4) thus provoking the above question. The quantity R_δ, given by

$$R_\delta = \frac{\rho U_b}{\mu} \frac{d\delta}{dx} \frac{U_a + U_b}{U_a - U_b}$$

is found to be nearly identical between cases 1 and 5 and between cases 2 and 4 for a given convective Mach number. The streams that form the mixing layer are both air in these cases. This leads to the speculation that in order to have equivalence between two mixing layers, the parameter R_δ must also be considered which is a Reynolds number like parameter for mixing layer.

As mentioned earlier, the computations were sensitive to the initial distributions of the turbulence field. However, the free stream turbulence level does not affect the predicted characteristics of the mixing layer significantly. The compressibility correction term is dependent upon the local turbulent Mach number as defined in equation(31). The magnitude of this term reaches a maximum value approximately equal to one-third the dissipation rate (ϵ) inside the mixing layer. This indicates that the two-equation model without any correction for the effects of compressibility will be grossly in error in predicting compressible flows.

Figures 10 - 12 show the results obtained for a reacting turbulent mixing layer using the model described in this paper. Hydrogen-oxygen reaction is modelled by means of a 18-reaction steps, 9-species system in these calculations. The free stream velocities, pressure and temperature are identical between the two cases. The free stream temperature is 2000 K and the pressure is 1 atm. Comparison between reacting and nonreacting cases are shown in figures 10 and 11. Figure 10 shows the width of the mixing layer for a supersonic convective Mach number. Figures 11 are the mean temperature, axial velocity and turbulent kinetic energy distributions. Examination of these figures indicates that the temperature distribution is altered, as expected, due to the heat release during the chemical reactions. The temperature reaches a peak value of about 2510 K inside the mixing layer. However, the mean dynamic and turbulence fields do not change. The width of the shear layer remains almost constant. Figure 12 shows the distributions of the primary species in the flow. Mass concentrations of hydrogen, oxygen and water vapor are shown. The extent of the reaction zone can be seen clearly here.

CONCLUDING REMARKS

A two-equation turbulence model $(k - \epsilon)$ has been modified to be suitable for addressing compressible flows. A compressibility correction model based on modelling the dilatational terms in the Reynolds stress equations has been used. A two-dimensional high-speed mixing layer is studied using the model. Comparisons of the predictions with available experimental data and the predictions of a compressible Reynolds stress closure indicate that the model is well suited for the study of such flows. The decrease in the growth rate of the mixing layer with increasing convective Mach number is well predicted by the model. A parameter which may be useful to establish the equivalence of mixing layers has been identified. Representative solutions of reacting high-speed mixing layers also have been given. This two-equation model is being developed for application to reacting, compressible flows.

ACKNOWLEDGMENTS

References

[1] Drummond, J. P.; Carpenter, M. H.; and Riggins, D. W., "Mixing and Mixing Enhancement in Supersonic Reacting Flows", *High Speed Propulsion Systems: Contributions to Thermodynamic Analysis*, ed. E. T. Curran and S. N. B. Murthy, American Institute of Astronautics and Aeronautics, Washington, D. C., 1990.

[2] Drummond, J. P.; and Weidner, E. H., "Numerical Study of a Scramjet Engine Flowfield", *AIAA J.*, vol. 20, no. 9, Sept. 1982, pp. 1182–1187.

[3] Nallasamy, M., "Turbulence Models and Their Applications To The Prediction of Internal Flows, A Review", *Computers & Fluids,* vol. 15, no. 2, 1987, pp. 151–194.

[4] Yang, Z.Y.; Chin, S.B. and Swithenbank, J., "On The Modelling of The k-Equation For Compressible Flow", Dept. of Mechanical and Process Engg., University of Sheffield, U.K. To be published.

[5] Sarkar, S.; Erlebacher, G.; Hussaini, M. Y.; and Kreiss, H. O., "The Analysis and Modeling of Dilatational Terms in Compressible Turbulence", *NASA CR* 181959, 1989.

[6] Favre, A., "Statistical Equations of Turbulent Gases", *Institut de Mechanique Statistique de la Turbulence, Marseille.*

[7] Jones, W.P. and Launder, B.E., "The Prediction of Laminarization with a Two-Equation Model of Turbulence", *Int. J. Heat Mass Transfer*, Vol.15, 1972, pp 301-314.

[8] "Free Turbulent Shear Flows", *NASA SP-321*, Vol.1, 1972.

[9] Brown, G. L.; and Roshko, A., "On Density Effects and Large Structure in Turbulent Mixing Layers", *J. Fluid Mech.,* vol. 64, pt. 4, 1974, pp. 775–816.

[10] "Seventh Symposium on Turbulent Shear Flows", Vol.1 and 2 Stanford University, Stanford, California, 1989.

[11] Papamoschou, D. and Roshko, A., "The Compressible Turbulent Shear Layer : An Experimental Study", *J.Fluid Mechanics*, v.197, 1988, pp 453-477.

[12] Carpenter, M. H., "Three-Dimensional Computations of Cross-Flow Injection and Combustion in a Supersonic Flow", AIAA-89-1870, June 1989.

[13] Sarkar, S. and Balakrishnan, L., "Application of a Reynolds Stress Turbulence Model to the Compressible Shear Layer", *ICASE Report* 90-18, 1990.

[14] Balakrishnan, L., Old Dominion University, Private communication.

[15] Birch, S.F. and Eggers, J.M., "A Critical Review of the Experimental Data for Developed Free Turbulent Shear Layers", *NASA SP*-321, 1973, pp 11-40.

[16] Ikawa, H. and Kubota, T., "Investigation of Supersonic Turbulent Mixing Layer with Zero Pressure Gradient", *AIAA Journal*, Vol.13, 1975, pp 566-572.

[17] Wagner, R.D., "Measured and Calculated Mean-Flow Properties of a Two-Dimensional, Hypersonic, Turbulent Wake", *NASA TN* D-6927, 1972.

[18] Williams, F. A.; *Combustion Theory.* Addison-Wesley Publishing Company, Inc., Reading, MA, pp. 358-429, 1965.

[19] Launder, B.E.; Reece, G.J. and Rodi, W., "Progress in the Development of a Reynolds Stress Turbulence Closure", *J. Fluid Mech.*, Vol.68, 1975, pp 537-566.

[20] Strahle, W.C., "Velocity-Pressure Gradient Correlation in Reactive Turbulent Flows", *Combustion Science and Technology*, Vol.32, 1983, pp 289-305.

[21] Drummond, J. P.,"A Two-Dimensional Numerical Simulation of a Supersonic, Chemically Reacting Mixing Layer", *NASA TM* 4055, 1988.
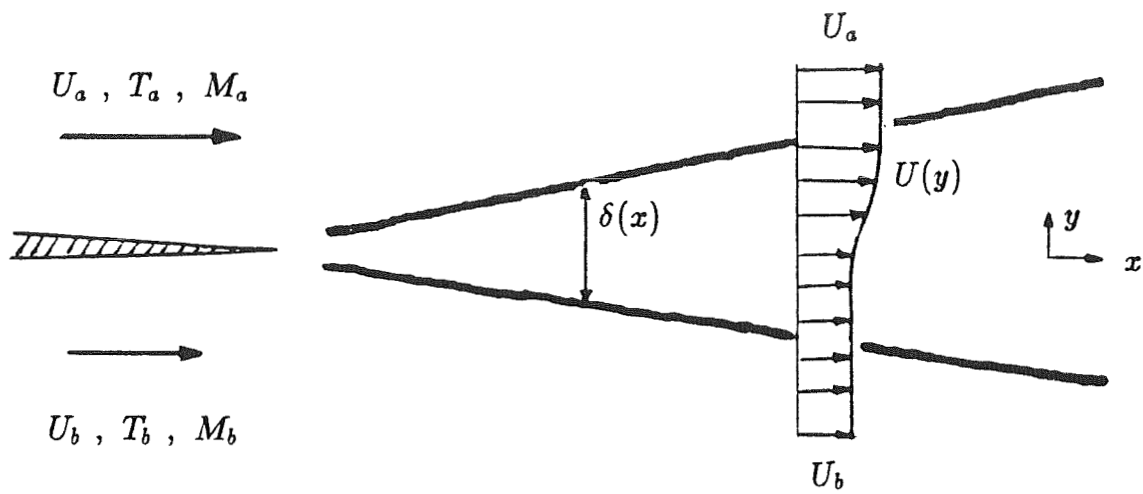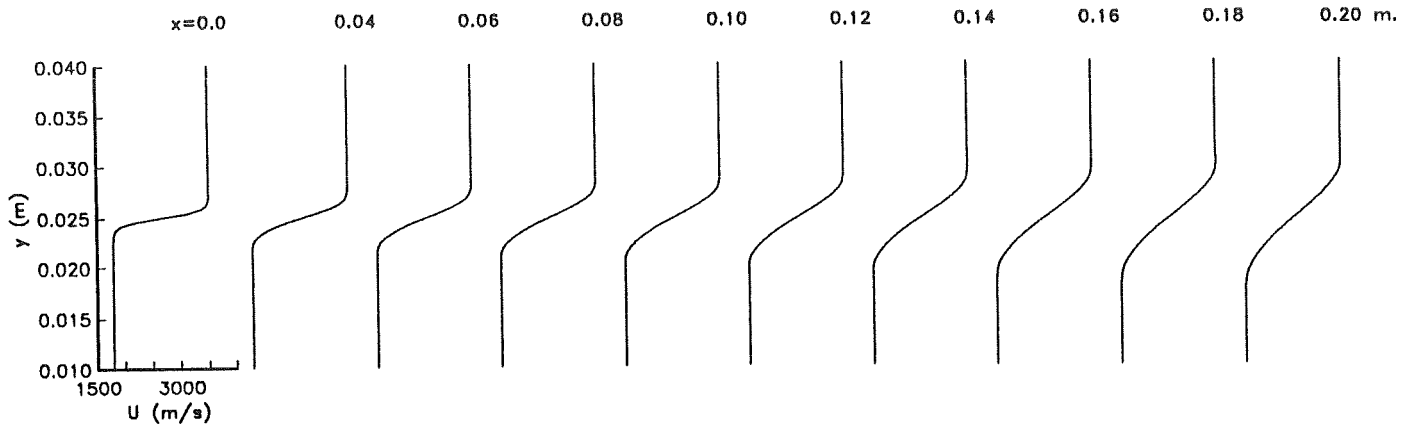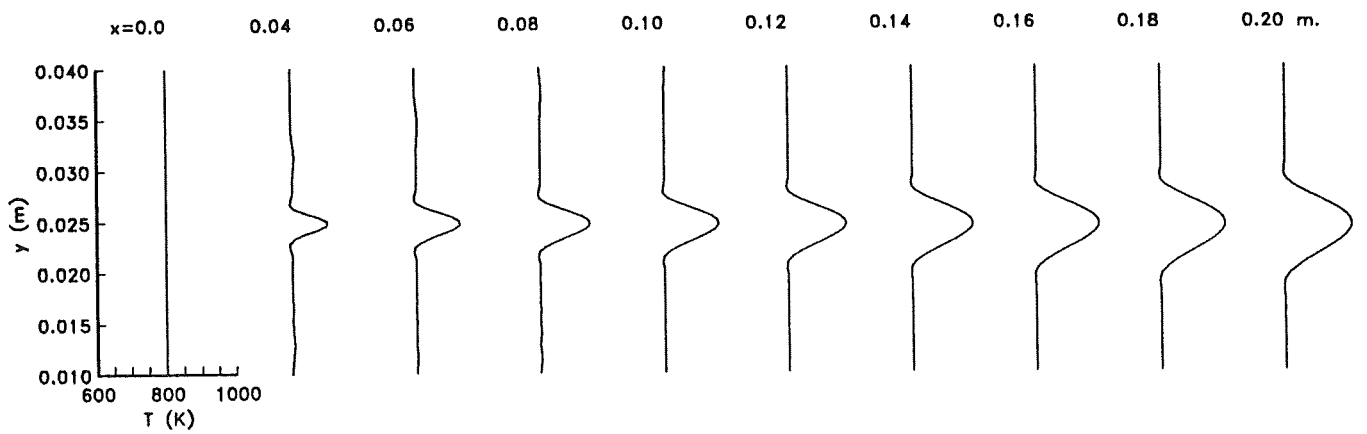
Fig.1 Mixing Layer (schematic)

Fig.2 Initial Profiles

x=0.0   0.04   0.06   0.08   0.10   0.12   0.14   0.16   0.18   0.20 m.

a) Mean Axial Velocity

b) Mean Temperature

c) Turbulent Kinetic Energy

M_c=1.5 , α=1.0 , T_∞=800 K
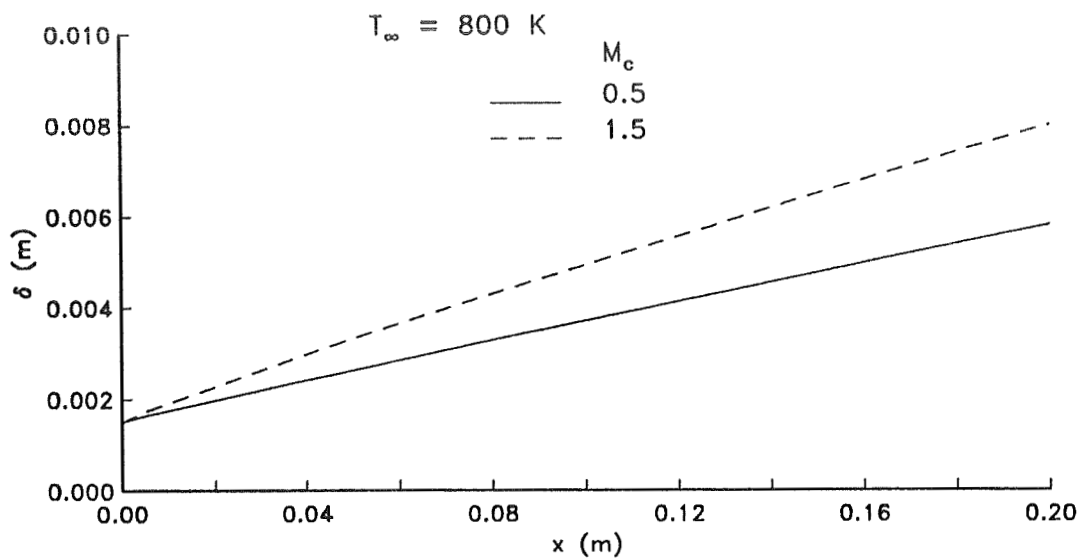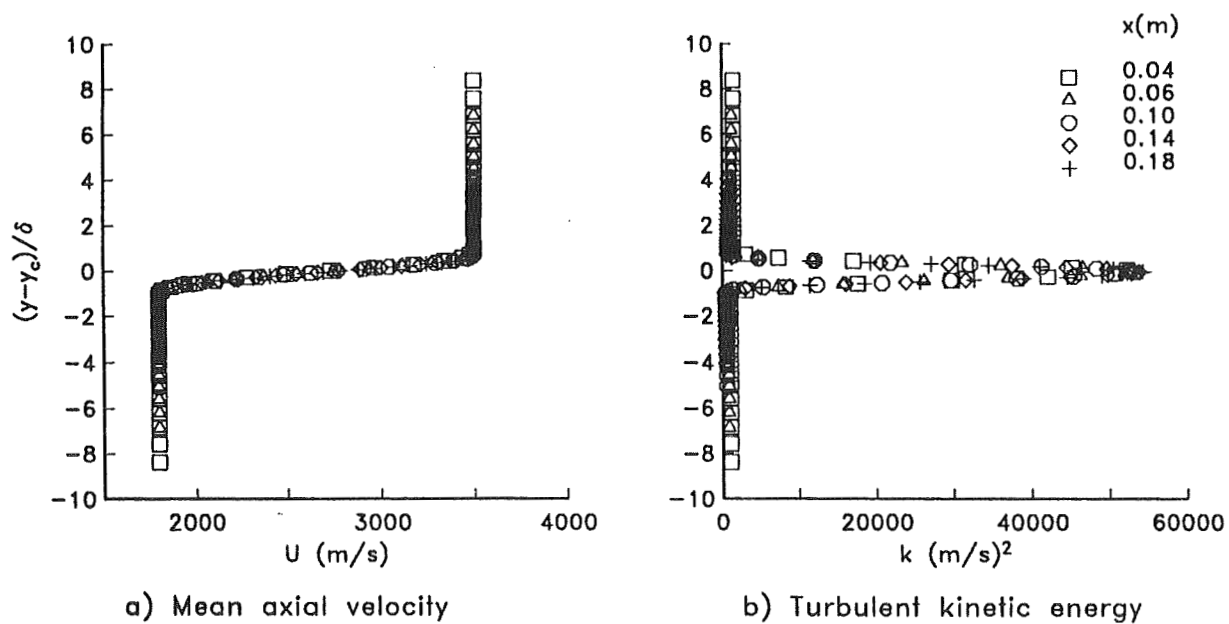
Fig.3 Predicted Flow Field of Mixing Layer

422

$$\delta = (U_a - U_b)/(\partial u / \partial y)_{max}$$

Fig.4 Mixing Layer Thickness

a) Mean axial velocity

b) Turbulent kinetic energy

$$M_c = 1.5, \quad \alpha = 1.0, \quad T_\infty = 800 \ K$$

Fig.5 Mixing Layer Similarity Profiles
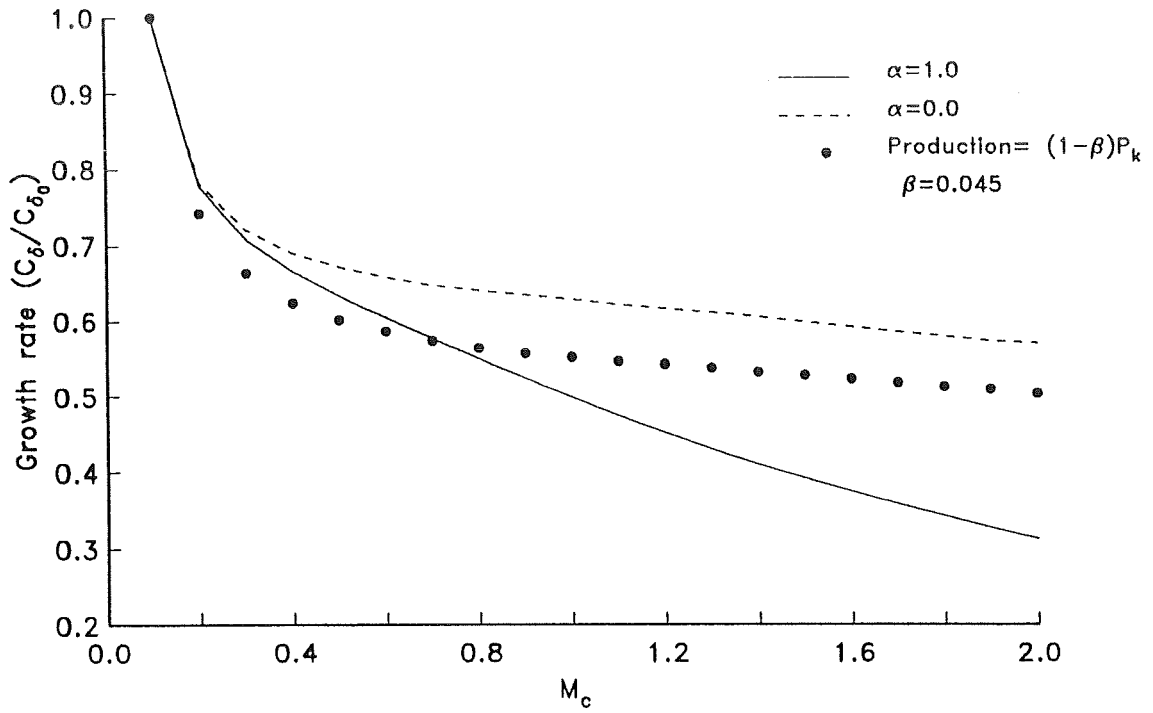
Fig.6 Effect of compressibility correction
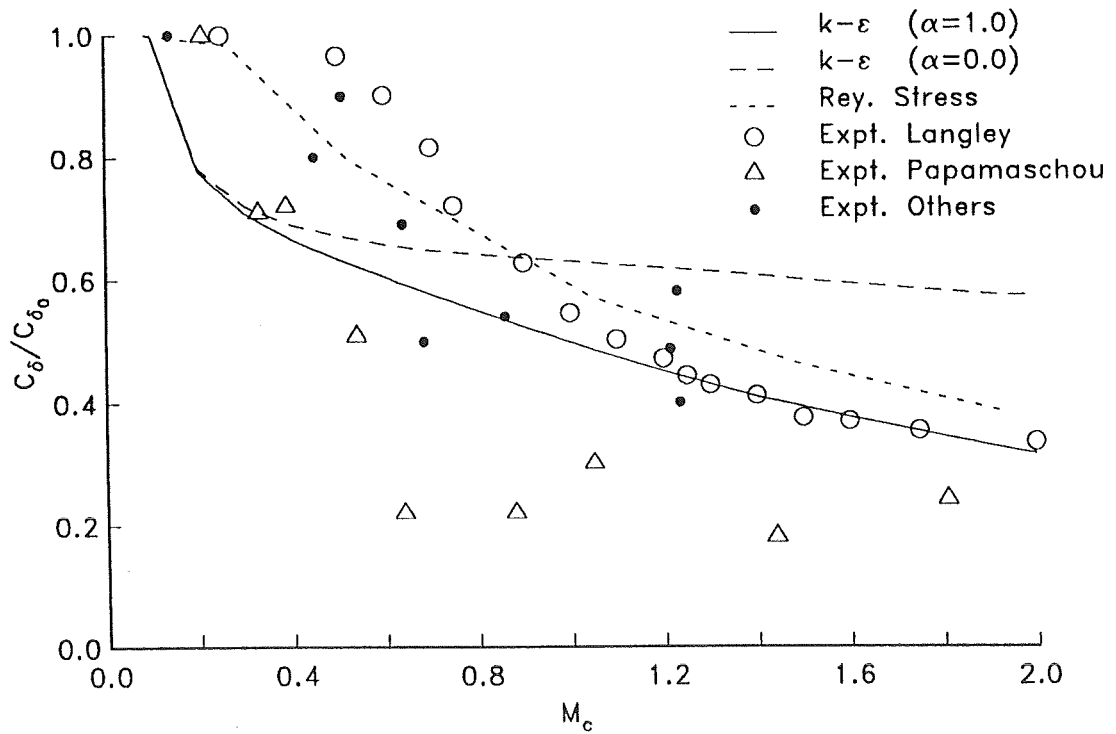
Fig.7 Comparison of growth rate data
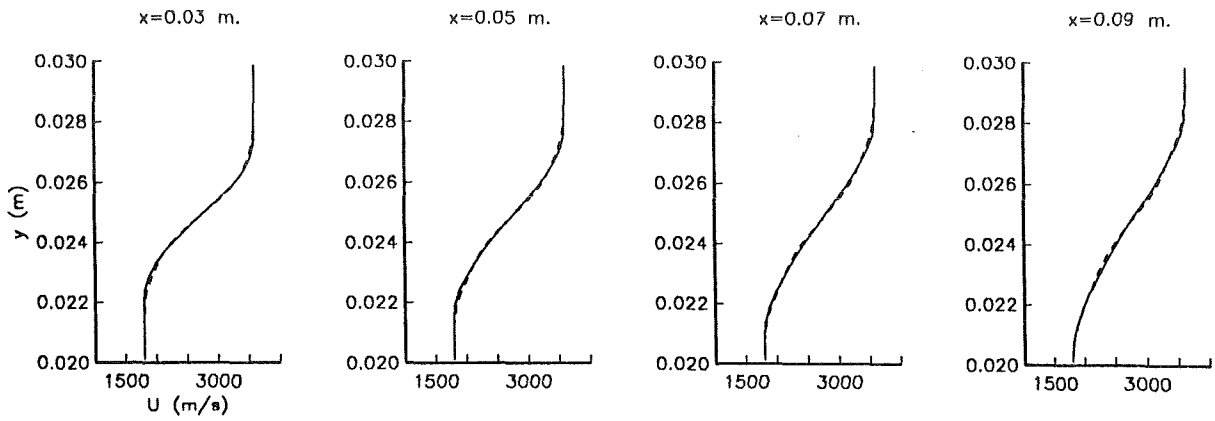
a) Mean Axial Velocity
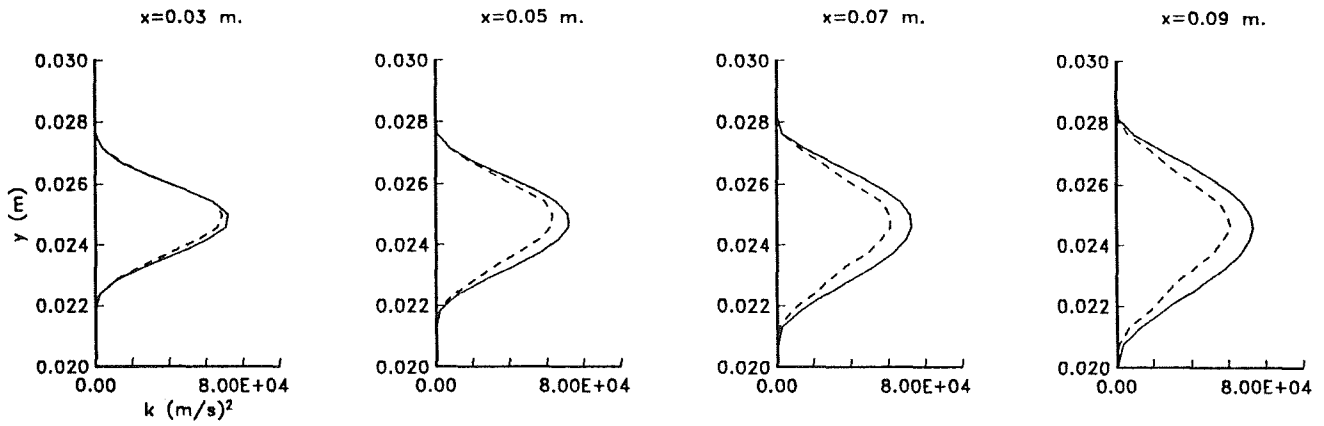
b) Turbulent Kinetic Energy
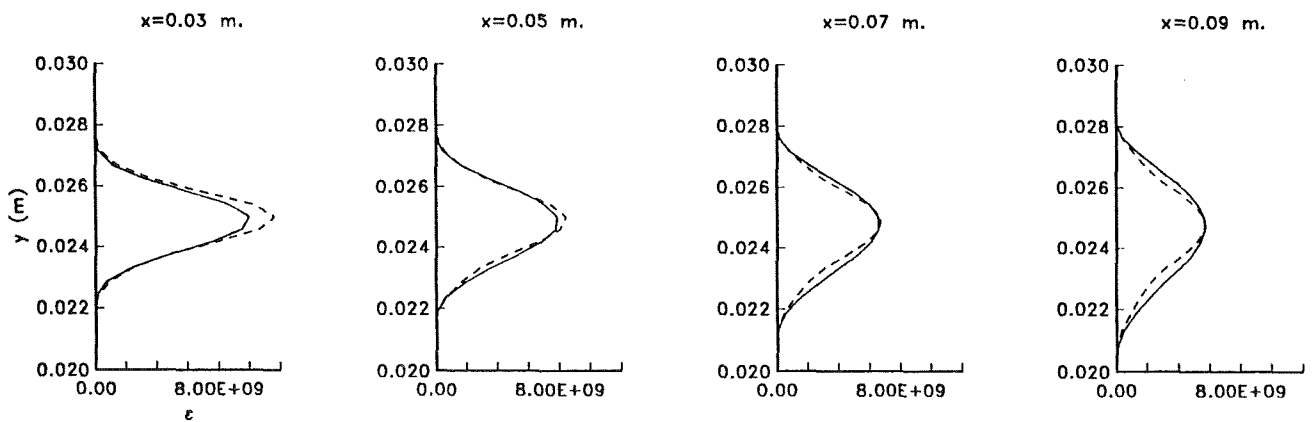
c) Dissipation Rate

$T_\infty=2000$ K, $M_c=1.0$ $\alpha=1.0$

———— k—ε
----- Rey. Stress

Fig.8 Comparison Between k—ε and Reynolds Stress Closures
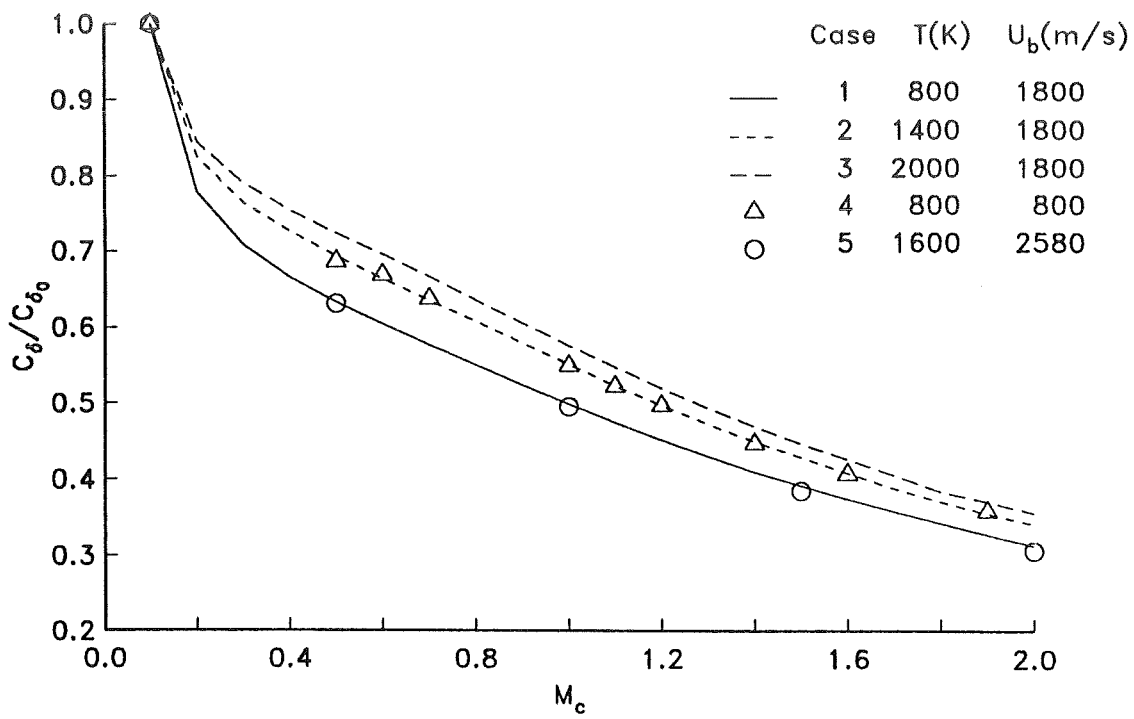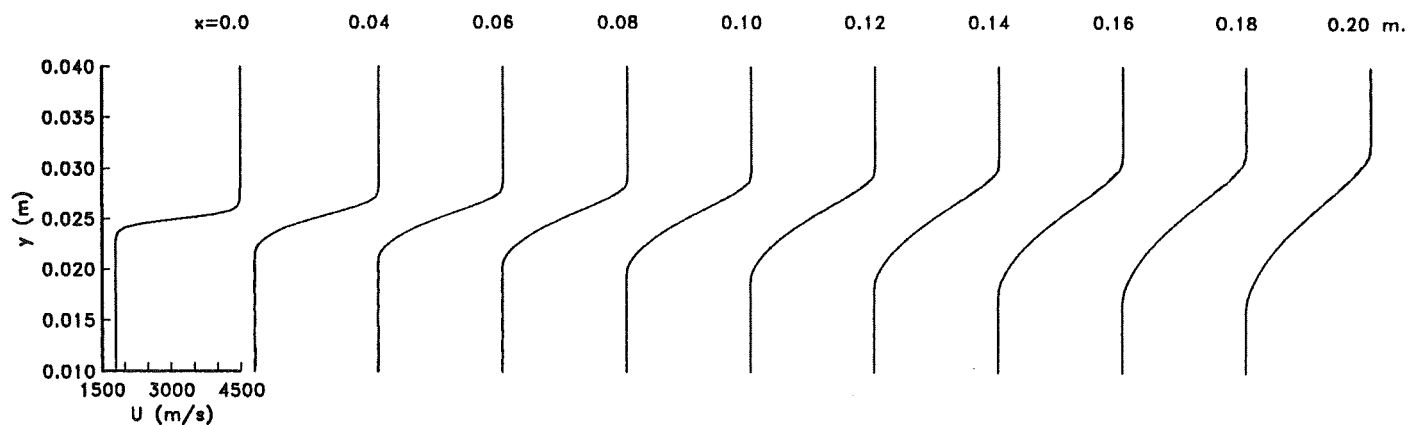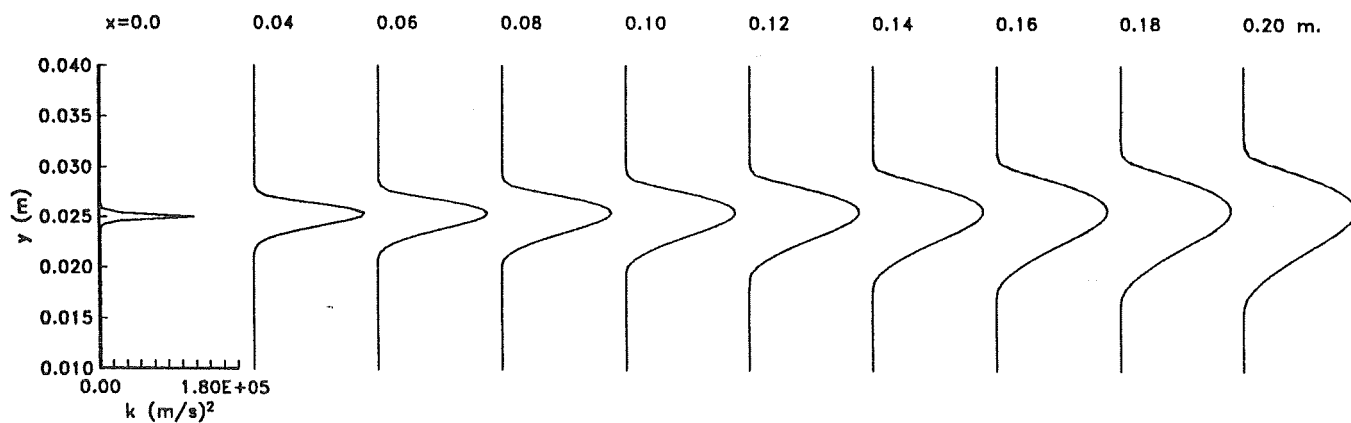
Fig.9 Effect of Temperature on Growth Rate
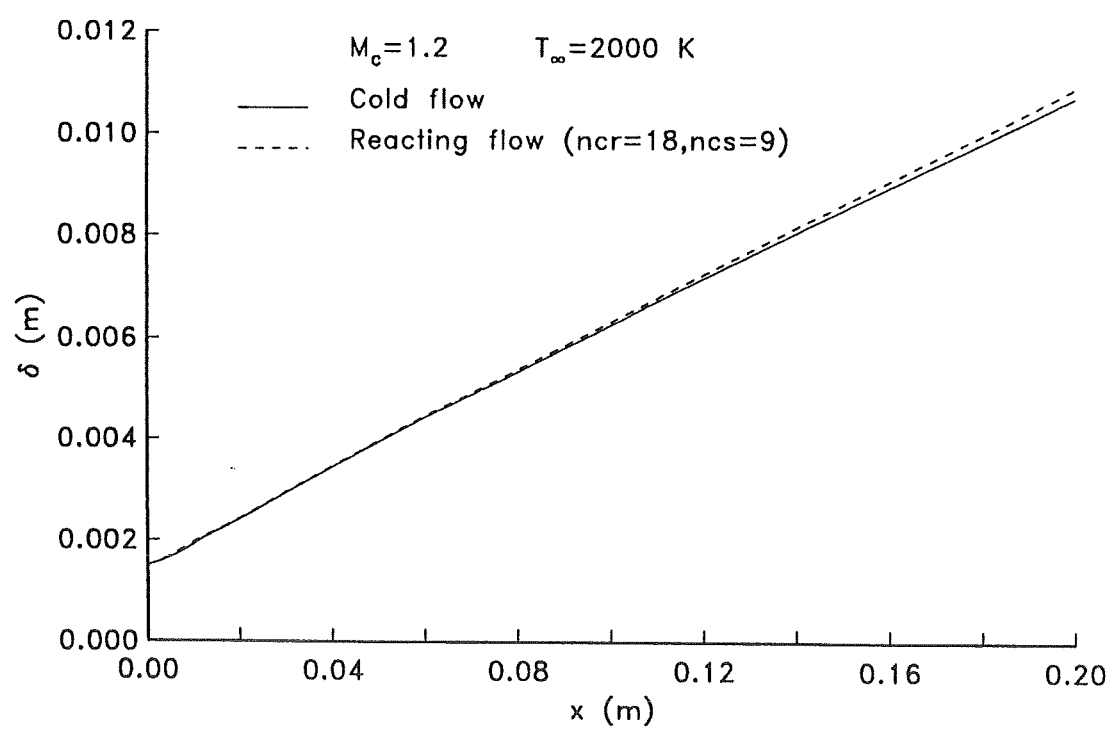
Fig.10 Effect of Reactions on Mixing Layer Growth
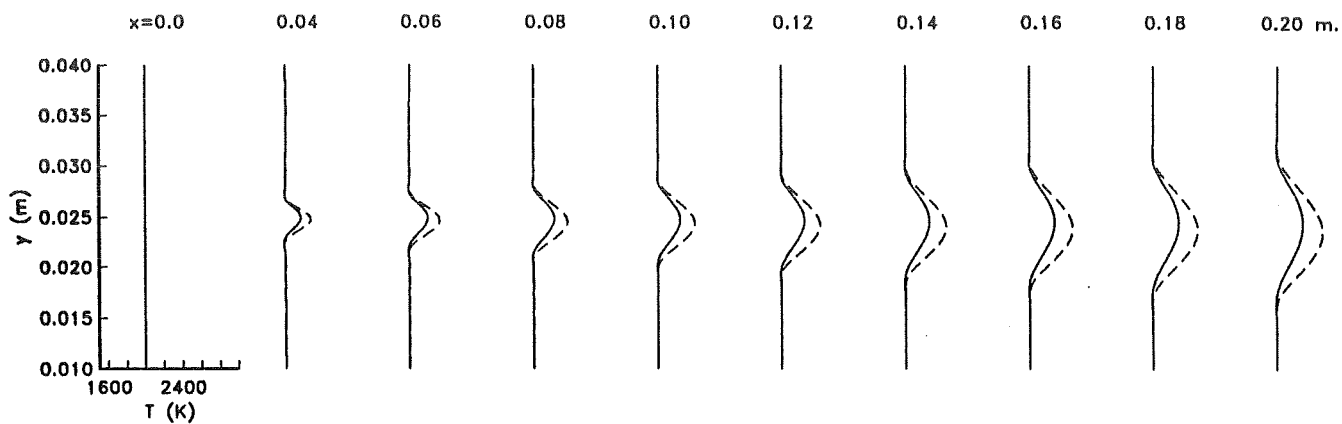
a) Mean Temperature

b) Mean Axial Velocity

c) Turbulent Kinetic Energy

_____ Cold flow

---- Reacting flow

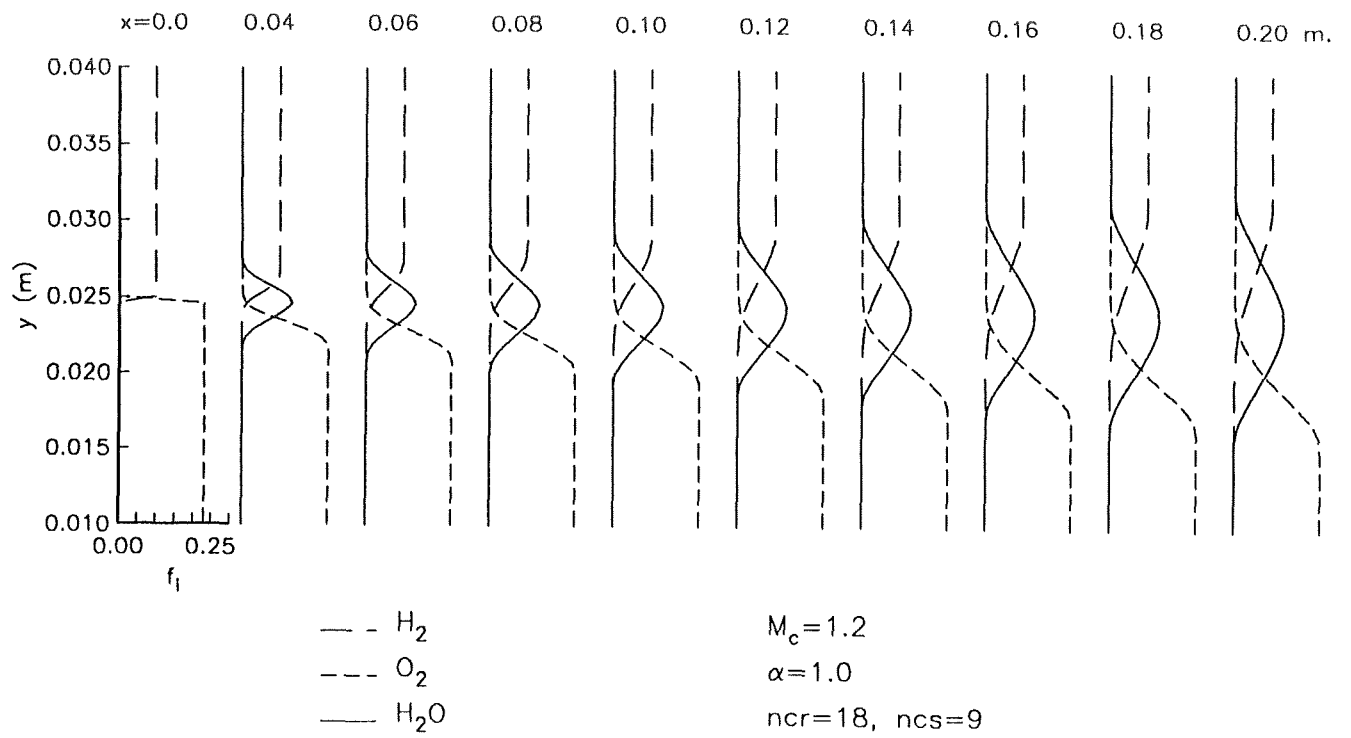$M_c = 1.2$, $\alpha = 1.0$, $T_\infty = 2000$ K

Fig.11 Effect of Chemical Reactions on Mixing Layer

Fig.12 Species Mass Fractions